



Wales, C. J. A., Jones, D. P., Gaitonde, A. L., Risley-Settle, P., & Peace, A. (2022). Comparison of Aircraft Loads Using URANS and Actuator Disk Modelling of Propellers. In *AIAA Aviation 2022: Session: Propeller/Rotorcraft/Wind Turbine Aerodynamics I* [AIAA 2022-3684] American Institute of Aeronautics and Astronautics Inc. (AIAA).  
<https://doi.org/10.2514/6.2022-3684>

Peer reviewed version

Link to published version (if available):  
[10.2514/6.2022-3684](https://doi.org/10.2514/6.2022-3684)

[Link to publication record in Explore Bristol Research](#)  
PDF-document

This is the author accepted manuscript (AAM). The final published version (version of record) is available online via AIAA at <https://arc.aiaa.org/doi/abs/10.2514/6.2022-3684> Please refer to any applicable terms of use of the publisher.

## University of Bristol - Explore Bristol Research

### General rights

This document is made available in accordance with publisher policies. Please cite only the published version using the reference above. Full terms of use are available:  
<http://www.bristol.ac.uk/red/research-policy/pure/user-guides/ebr-terms/>

# Comparison of Aircraft Loads Using URANS and Actuator Disk Modelling of Propellers

Christopher Wales<sup>\*</sup> Dorian J. Jones<sup>†</sup> and Ann L. Gaitonde<sup>‡</sup>  
*University of Bristol, Bristol, BS8 1TR, United Kingdom*

Peter Risley-Settle<sup>§</sup> and Andrew J. Peace<sup>¶</sup>  
*Aircraft Research Association Ltd., Bedford, United Kingdom, MK41 7PF*

**A comparison of simulations are performed using both steady RANS with an actuator disk model to represent the propellers and URANS with full rotating blade geometry, for the Clean Sky 2 flying test bed 2, which is a regional turboprop with co-rotating propellers. The simulations are performed for a cruise configuration at Mach 0.2 and a Reynolds number of  $11.933 \times 10^6$  for a range of angles of attack and side slip angles. The generation of the database for the actuator disk model is explained, along with the calibration of the blade angle to give a specified thrust. Aerodynamic coefficients for both the airframe and the propellers are extracted and compared with wind-tunnel data from an atmospheric wind-tunnel test undertaken in a previous Clean Sky 2 project (ReLOAD).**

## I. Introduction

The increased emphasis on improved aircraft efficiency through reduced fuel burn, as reflected in the European ACARE targets in Horizon 2020, has encouraged the aerospace industry to consider alternative propulsion systems to the conventional turbofan. In particular, a renewed interest in turboprop-driven regional aircraft has emerged. The wake from the propellers can have a large effect on the aircraft forces and moments. This paper will describe the work done as part of the Clean Sky 2 PERTURB (Power Effects aerodynamics for a Regional TURBoprop) project, modelling the power on loads for the for the Clean Sky 2 flying test bed demonstrator, shown in Figure 1.

Two different CFD approaches have been used within PERTURB to model the effect of the propellers on the aircraft loads. The first approach is perform URANS simulations with the propeller blades fully modelled. For detailed blade modelling, the main challenges switch from those of flow solver approach to those of meshing approach. A rotating propeller co-exists with a static airframe, immediately implying that the mesh has a rotating part fixed with the rotating blades and a static part fixed with the airframe. The issue then becomes how these two parts interface together. There are two choices: a sliding interface approach whereby the fixed and rotating meshes do not overlap but abut each other; and a Chimera approach whereby the meshes overlap each other. The latter has been used in the work.

Using unsteady CFD to model the full aircraft with the installed propeller blade geometry offers a high fidelity option for calculating aircraft and propeller loads. With a time step that is small enough to accurately model the propeller physics and the requirement to simulate enough time for the propeller wake to reach the tail of the aircraft, this approach is computationally expensive. This means that performing a large number of these simulations are not computationally affordable, so a lower cost approach is required. As the details of the aerodynamics of the individual blades is not the focus of this project and the main interest is the effect of the propeller on the aircraft loads, then it is possible to use an actuator disk modelling approach. As this only requires running steady CFD, this requires significantly less computational cost. In the work below the cost and accuracy of the actuator disk approach is compared to modelling the full propeller geometry using unsteady RANS. The disk model is driven by a propeller performance database, which has been created using 2D CFD simulations of propeller blade sections.

Both approaches can be used to calculate the 1P forces and moments for the airframe and props. This paper compares the airframe aerodynamic coefficients, propeller thrust and torque predicted using URANS with the fully modelled propeller blades against the steady actuator disk model, for a range of angles of attack and side slip. Additionally, the

---

<sup>\*</sup>Research Associate, Department of Aerospace Engineering

<sup>†</sup>Professor of Aerodynamics, Department of Aerospace Engineering

<sup>‡</sup>Professor of Aerodynamics, Department of Aerospace Engineering

<sup>§</sup>Senior aerodynamics engineer, Aerodynamics Department, ARA.

<sup>¶</sup>Chief Scientist, ARA

CFD simulations are compared to with wind-tunnel data from an atmospheric wind-tunnel test undertaken in a previous Clean Sky 2 project ReLOAD (Regional turboprop loads control through active and passive technologies)[1].



**Fig. 1 PERTURB regional turboprop aircraft**

## **II. CFD methodologies**

### **A. Overall methodology**

The DLR-developed TAU flow solver in RANS mode was used for all flow simulations[2]. TAU is a finite-volume vertex-based solver with a broad range of modelling and numerics functionality. All simulations herein used second-order spatial schemes. The steady RANS solutions employed the central variant, while the unsteady RANS solutions employed the TAU-recommended upwind variant (AUSMDV) which proved a more stable option for these cases. More details of each approach are given below.

### **B. Steady RANS actuator disk approach**

Propellers generate thrust due to aerodynamic forces acting on the surface of rotating blades. As a consequence reaction forces act on the fluid which increase the momentum and the energy of the flow. The actuator disk approach is based on modelling the propeller as a zero-thickness circular disk which applies the equivalent time-averaged thrust and swirl imparted to the fluid by the propeller. As the disk properties are time-averaged, over a single revolution of the propeller, the intrinsically unsteady nature of the simulation problem is removed. Therefore, steady RANS modelling can be used, giving a significant reduction in compute time compared to an unsteady simulation.

The actuator disk is driven by a distribution of radially-and azimuthally-varying three-component force vectors on the disk, representing the time-averaged force imparted by the propeller on the fluid. However, these quantities will not in general be known. These can be approximated by using the blade section lift and drag coefficients, which vary with disk radius, along with the details of both local chord, twist and local effective flow angle along the blade from root to tip. By including this variation, the interference of the airframe on the disk and also free-stream incidence effects can be more faithfully modelled. This functionality is available in TAU through the specification of sectional lift and drag polars at each radial blade position, again along with local twist and local chord[3]

The actuator disk model in TAU [4] is driven by a database which specifies propeller blade sectional lift and drag coefficient as a function of local onset incidence, for a number of radial stations along the blade. This can be from experimental data or as in this case from a database of two-dimensional RANS simulations for each blade section. To generate the required data for the disk models, ten radial sections were taken from the propeller blade. 2D RANS simulations, using the Spalart Allmaras negative model [5], were then performed using TAU for each of these sections for a range of incidences (zero incidence equates to flow parallel to the section chord line) and the lift and drag coefficient were extracted. The Spalart Allmaras negative turbulence model was also used the RANS actuator disk simulations. The sectional Mach number and Reynolds number used was calculated from the freestream Mach number and the rotational speed at each section of the blade. This assumes that the polar is not sensitive to changes in local Mach

number due to interference effects. However, this approximation is not felt to be significant in the context of the overall approximation of the actuator disk approach.

Although it is expected that the local onset flow angle to each blade section is small and hence in the linear regime, transient behaviour during the CFD convergence process may result in incidences outside the linear range. For incidences near and beyond maximum lift, i.e. when some flow separation has occurred, the raw lift and drag polars were not sufficiently smooth to provide data for the actuator disk. Hence, at these incidences the polars were smoothed by hand using expert judgement.

### C. URANS blade modelling approach

The overall URANS approach consists of performing a number of time steps with TAU in unsteady mode, with each time step corresponding to an increment in propeller rotation, i.e. the overlapping mesh block rotates by an increment in azimuthal angle. As each propeller has six blades, a blade passes a fixed point every  $60^\circ$ . A time step equating to  $5^\circ$  rotation was chosen to give acceptable accuracy in propeller aerodynamics for this situation[6]. Hence, one rotation corresponded to 72 time steps.

In contrast to the steady RANS approach, the  $k-\omega$  SST turbulence model was used for URANS. Consistent with URANS being the high-fidelity modelling approach in the project, it was felt this choice would give a better detailed representation of the propeller tip vortices and their interaction with the airframe. The dual time-stepping scheme was used in TAU. A successful simulation is deemed to have occurred when a quasi-steady state is reached, i.e. when key aerodynamic quantities do not change for additional complete rotations of the propellers. A quasi-steady state for the URANS simulations was generally obtained after six complete rotations of the propellers. Such a state was observed to have occurred more rapidly than this on the main wing downstream of the propellers, but the aircraft pitching moment did not stabilise until after the propeller wakes reached the horizontal tail plane. Simulations were run for longer to confirm that a steady state had been reached. This also gave several blade passes over which the data could be time-averaged to compare to the actuator disk model.

As will be seen the URANS needs to simulation a time that is long enough for the wake from the propellers to pass the tail plane. This in addition to the higher mesh size leads to the URANS requiring significantly more CPU runtime than the actuator disk model. The actuator disk model takes around 8500 CPU hours compared to around 276500 CPU hours for the URANS, per simulation. This approximately multiplies the number of CPU hours by 32 times per simulation.

### D. Meshing

Meshes were generated using the Solar mesher[7]. Due to both propellers spinning in the same direction all simulations required meshing of the full aircraft.

The meshing for actuator disk modelling is straightforward within the Solar meshing capability. The disk is defined as an additional component of geometry and mesh density is specified. The surface mesh on the disk is composed of quadrilaterals with a regular  $(r, \theta)$  structure. The disk itself has no grown layer mesh, and hence is largely surrounded by the far-field mesh; however, the near-field mesh on the spinner transfers smoothly onto the disk.

Meshes for the URANS blade modelling approach were generated using the Chimera (or over-lapping) mesh technique, wherein the complete mesh is composed of two parts: a background mesh, encompassing all of the geometry except the propeller blades and spinner; and a mesh block containing the propeller blades and spinner only. The former mesh has a void where the propeller would be and the latter mesh overlaps the former by a few mesh cells. In the flow solver, the overlapping mesh (both port and starboard) rotates at the appropriate rotation speed relative to the background mesh.

The Chimera background mesh is very similar to that used for the steady RANS simulations, although some refinement local to the overlapping, propeller block is necessary to ensure the mesh density in the overlap region is approximately the same for each mesh part, as required by the flow solver. The blade angle is calibrated to give a specified thrust coefficient. This necessitates extracting thrust for blade angle increments ( $0.5^\circ$ ) and then choosing the nearest increment to give the desired thrust. To do this using the fully-installed configuration would be expensive and time consuming, so a more approximate process should be undertaken, with the calibration performed using a simple isolated propeller model, using the actuator model described in section II.B. The same calibrated propeller pitch angle was used for both the RANS and URANS simulations.

The TAU flow solver possesses the required interpolation functionality for overlapping meshes. It is necessary to have a two-cell overlap and a similar mesh density in the overlap region, which poses a significant challenge in the

meshing phase. The propeller mesh tends to be very fine, which drives a similar local mesh density in the fixed, airframe mesh. Hence, the overall mesh is significantly bigger than that for the actuator disk approach, see Figure 2. Some mesh statistics are given in Table 1.

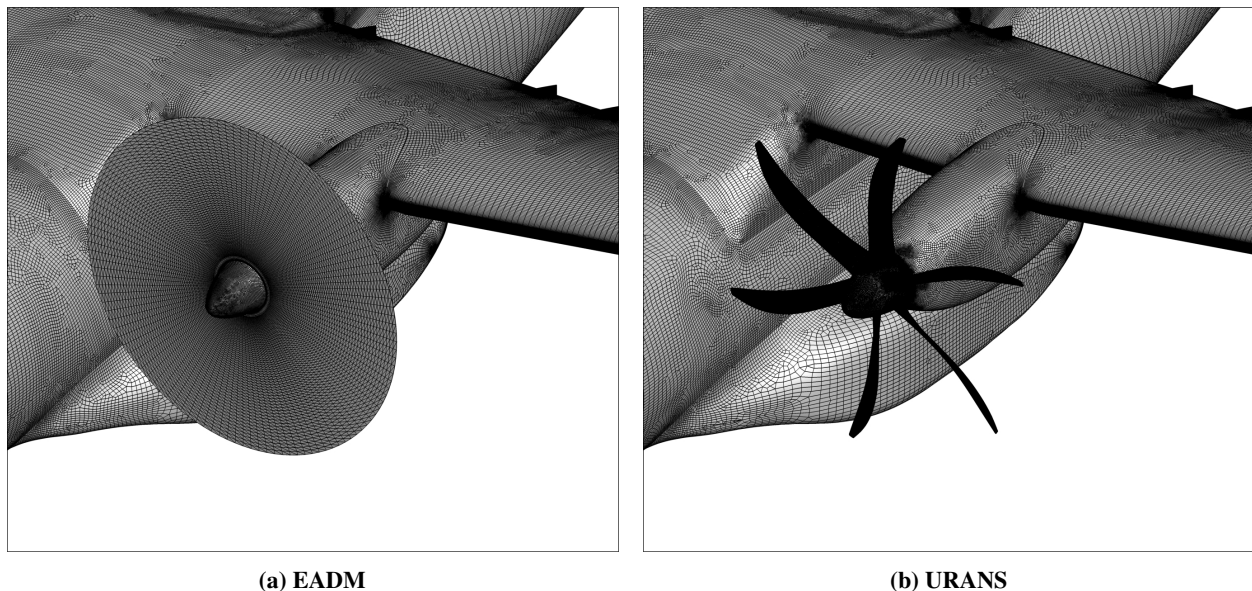


**Fig. 2 Comparison of surface meshes for EADM and URANS simulations for the cruise configuration**

	EADM	URANS
No. of elements	135,465,600	253,177,683
No. of points	50,947,614	117,474,377
No. of surface elements	1,119,933	2,515,050
Approximate CPU hrs taken	8500	276500

**Table 1 Comparison of mesh sizes and approximate simulation times**

### III. Results

The simulations were performed at the full aircraft scale, for a Mach number of 0.2 and a Reynolds number of  $11.933 \times 10^6$ . The actuator disk and URANS results are also compared to the experimental data obtained during the clean sky 2 ReLOAD project [1], which is at different Reynolds number  $1.43 \times 10^6$ . To be consistent with the experimental balance data the propeller loads include the spinner loads. The aircraft loads presented are without the propeller blade and spinner forces. The URANS loads presented are time average over one propeller rotation once a quasi-steady state had been reached. All forces coefficients are presented as percentage values relative to the URANS loads at zero degrees angle of attack and side slip, given by

$$\% \text{Coefficient} = \frac{\text{Coefficient} - \text{Coefficient}_{URANS}(\alpha = 0, \beta = 0)}{\text{Coefficient}_{URANS}(\alpha = 0, \beta = 0)} \quad (1)$$

The surface pressure distributions between the actuator disk model and the URANS at a  $12^\circ$  angle of attack, in Figure 3, show a good agreement between the two methods over the airframe. This includes the asymmetry of the wing pressure distribution due to the co-rotating propellers. The  $5^\circ$  side slip case, shown in Figure 4 also shows a good agreement in the surface pressures distribution with an increase asymmetry due to the additional side slip. Initially the vorticity shed from the propellers is preserved well, as shown in Figure 5. However, despite the number of cells used we can see

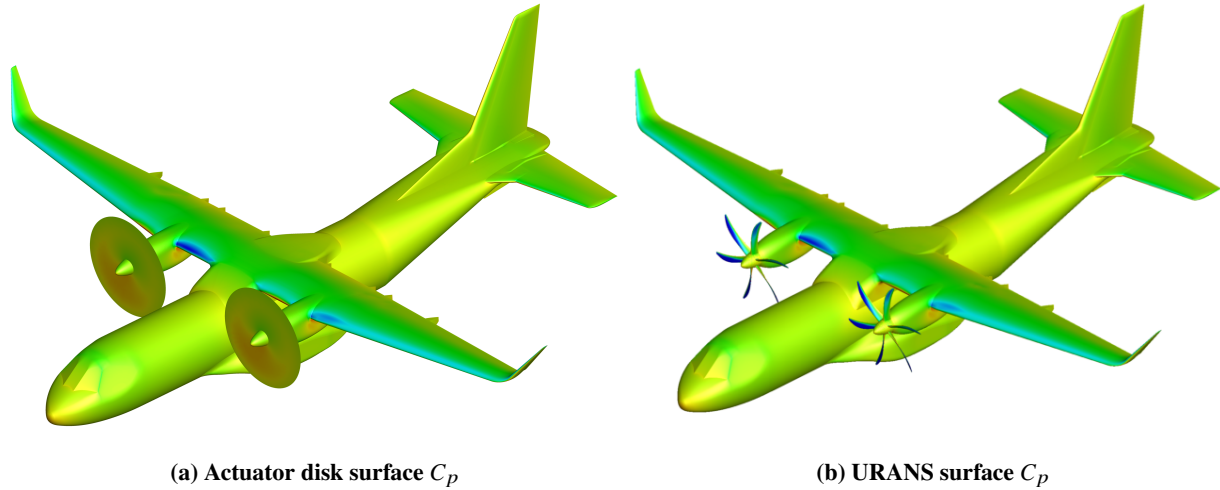


**Fig. 3 Comparison of surface  $C_p$ s between Actuator Disk Model and URANS (at  $t=0.316$  s), for  $12^\circ$  angle of attack**

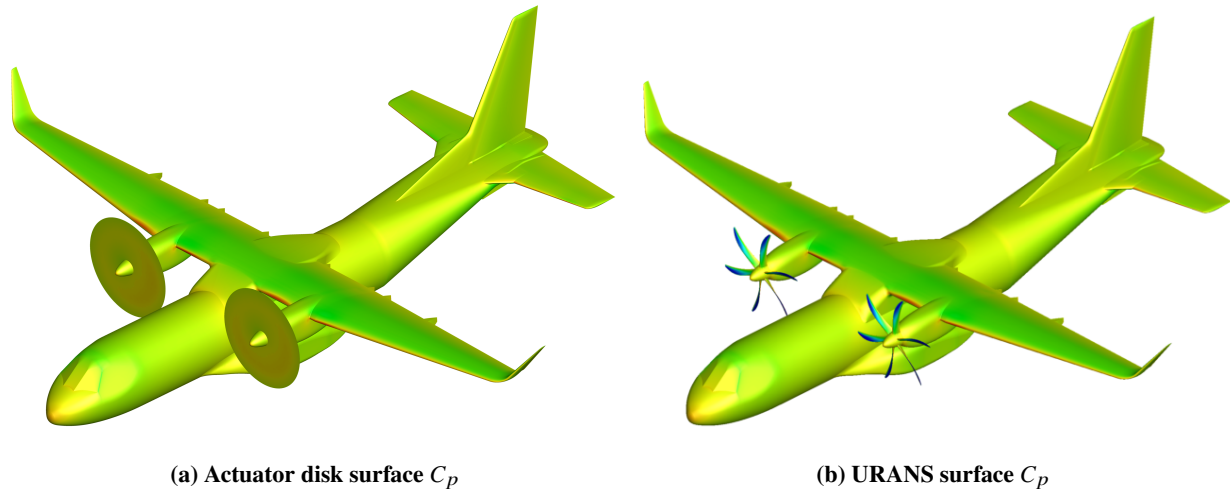


**Fig. 4 Comparison of surface  $C_p$ s between Actuator Disk Model and URANS (at  $t=0.316$  s), for  $5^\circ$  side slip**

some dissipation of the vortex core downstream. This is of particular interest when we consider the large overall change in integrated forces that the results show is associated with arrival of the propellers shed vorticity at the horizontal tail plane.

The incremental aircraft forces and moments at different angles of attack are shown in Figure 6. The actuator disk and URANS results show excellent agreement with each other. However, both approaches show an offset to the experimental data. For the drag and pitching moment the computational methods show similar trends with angle of attack. There is a slight difference in the lift curve slope for both methods compared to the experimental data and at the highest angle of attack both methods fail to capture the decrease in lift.

The incremental aircraft forces and moments at different side slip angles are shown in Figure 7. Once again the actuator disk model and the URANS results match closely and show similar trends with side slip. There is an offset in both methods for the lift but the moments match well.

The propeller thrust and torque plotted against angle of attack are shown in Figures 8 and 9, for the port and starboard propellers respectively. Both methods show similar predicted thrust at zero angle of attack. As incidence increases, the two methods show similar trends but difference between the methods increase at higher angles of attack. Both numerical approaches predict a higher thrust coefficient than the experiment, which could be associated with the blade angles being calibrated using an isolated propeller. There is an offset in the predicted torque between the actuator disk and

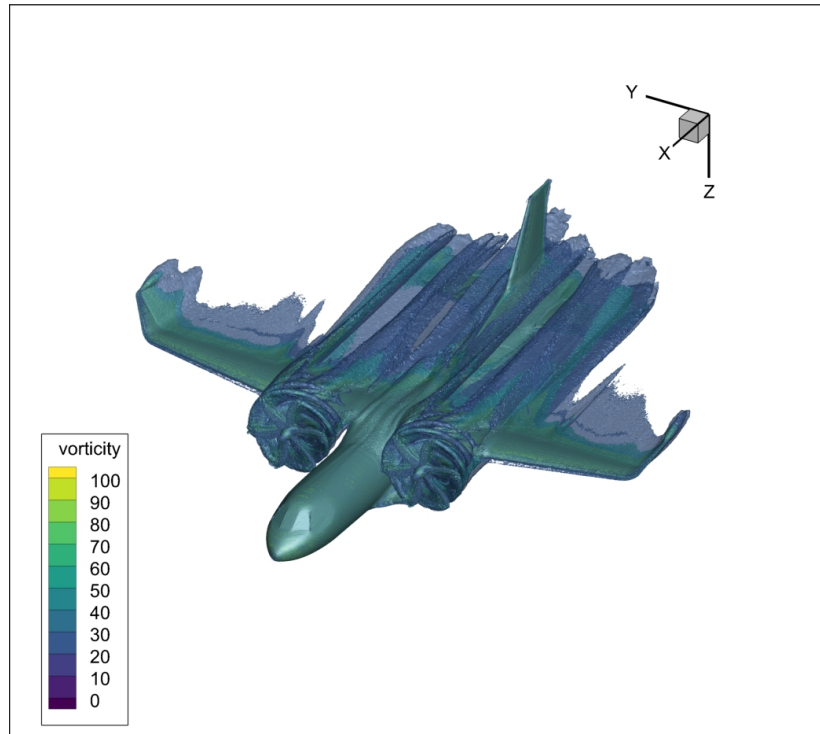


**Fig. 5 Vorticity contours at 12° angle of attack**

URANS but they show similar trends against angle of attack.

The propeller thrust and torque against side slip are shown in Figures 10 and 11, for the port and starboard propellers respectively. Both the actuator disk and URANS approaches match closely for the thrust variation with side slip at zero degrees angle of attack. Once again there is an offset to the experimental data but the trends match well. There is more of a difference in the predicted torque between the two methods but both show similar behaviour to the experimental data. Both methods correctly predict the different behaviour between the port and starboard propellers with varying side slip for thrust and torque.

### **A. Conclusion**

The URANS predictions generally agree well with the actuator disk predictions at full scale. For aircraft forces and moments, the agreement is very good, with some variation at the higher incidences. The latter observation could simply be due to the different turbulence model used for the two CFD fidelities (Spalart-Allmaras for actuator disk,  $k-\omega$  SST for URANS) and/or it could be due to the differing propeller modelling at the more severe conditions. For propeller forces and moments, the agreement is good for thrust and torque.

The level of agreement between the wind-tunnel data and the CFD characterisation is generally good, for both aircraft and propeller forces & moments. Comparison for aircraft rolling and yawing moment is excellent. Quantitative agreement is not as good for propeller thrust and torque, although the port-starboard variation is qualitatively predicted. This is because the propeller blade angle was calibrated to give a specified thrust using an isolated propeller model and it transpired that the installed thrust is higher than the isolated thrust.

### **Acknowledgments**

This work was carried out within the Clean Sky 2 research programme PERTURB, funded under grant number 831927. The authors gratefully acknowledge the support of Airbus Defence and Space. The URANS calculations presented were carried out using the computational facilities of the Advanced Computing Research Centre, University of Bristol - <http://www.bristol.ac.uk/acrc/>.

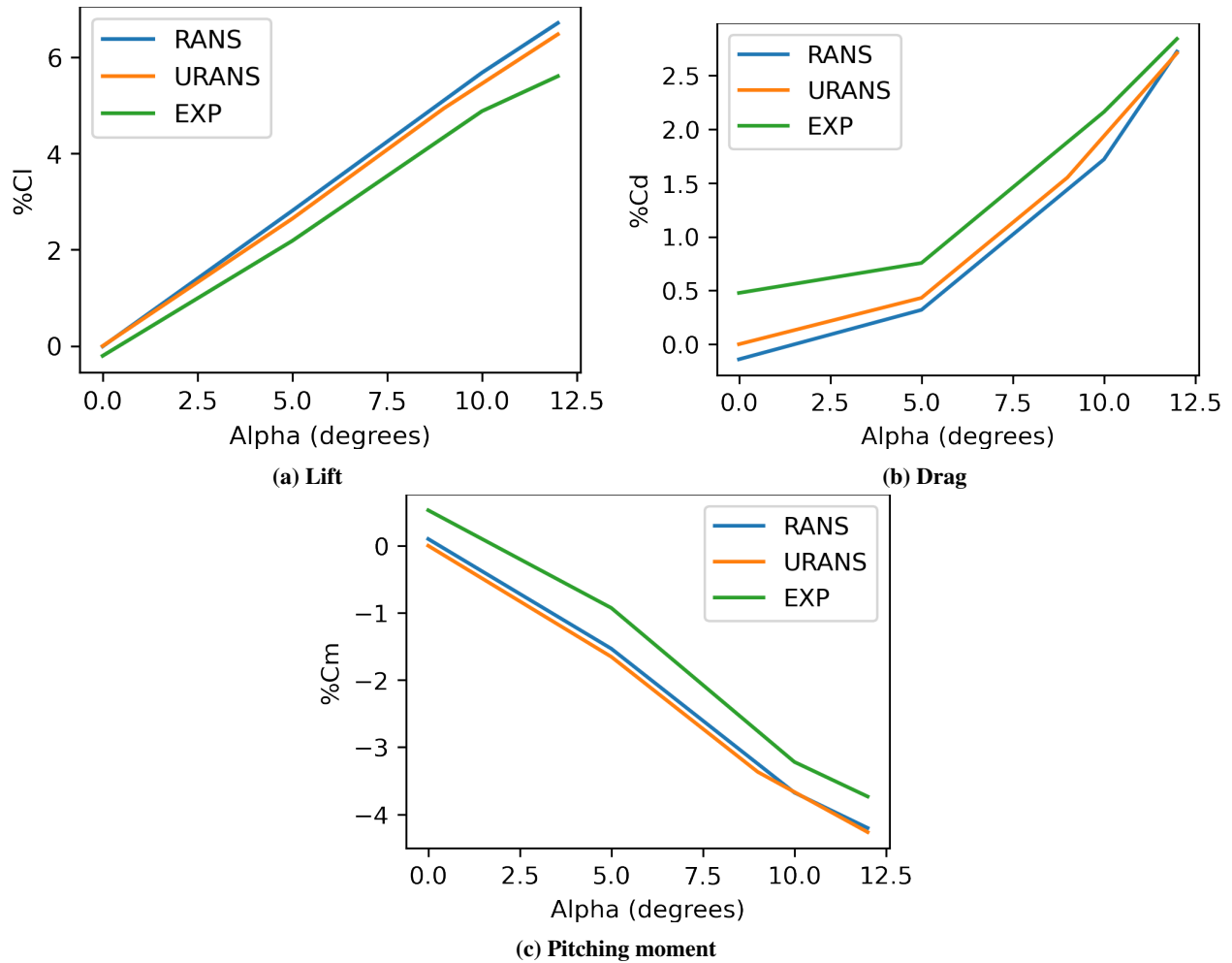


**Fig. 6** Difference in calculated force coefficients, relative to URANS results at angle of attack  $0^\circ$

## References

- [1] A, H., and J, P. A., "Characterisation of the low-speed handling qualities of a turboprop aircraft with deflected aileron and spoiler," Tech. rep., ARA Report RBC013/3, July 2018.
- [2] Schwaborn, D., Gerhold, T., and Heinrich, R., "The DLR TAU-code: Recent applications in research and industry," 2006.
- [3] Gutiérrez, C. M., Stuermer, A., Clemen, C., and Grimminger, A., *Validation of Actuator Disk Simulations of CROR Propulsion Systems at Low-Speed Flight Conditions*, 2012. <https://doi.org/10.2514/6.2012-2787>, URL <https://arc.aiaa.org/doi/abs/10.2514/6.2012-2787>.
- [4] *DLR TAU-code User Guide*, DLR, 2019.
- [5] Allmaras, S. R., and Johnson, F. T., "Modifications and clarifications for the implementation of the Spalart-Allmaras turbulence model," *Seventh international conference on computational fluid dynamics (ICCFD7)*, Vol. 1902, Big Island, HI, 2012.
- [6] Gomariz-Sancha, A., Maina, M., and Peace, A., "Analysis of propeller-airframe interaction effects through a combined numerical simulation and wind-tunnel testing approach," 2015. <https://doi.org/10.2514/6.2015-1026>.
- [7] Shaw, J. A., Stokes, S., and Lucking, M. A., "The rapid and robust generation of efficient hybrid grids for RANS simulations over complete aircraft," *International Journal for Numerical Methods in Fluids*, Vol. 43, No. 6-7, 2003, pp. 785–821. <https://doi.org/https://doi.org/10.1002/flid.497>, URL <https://onlinelibrary.wiley.com/doi/abs/10.1002/flid.497>.



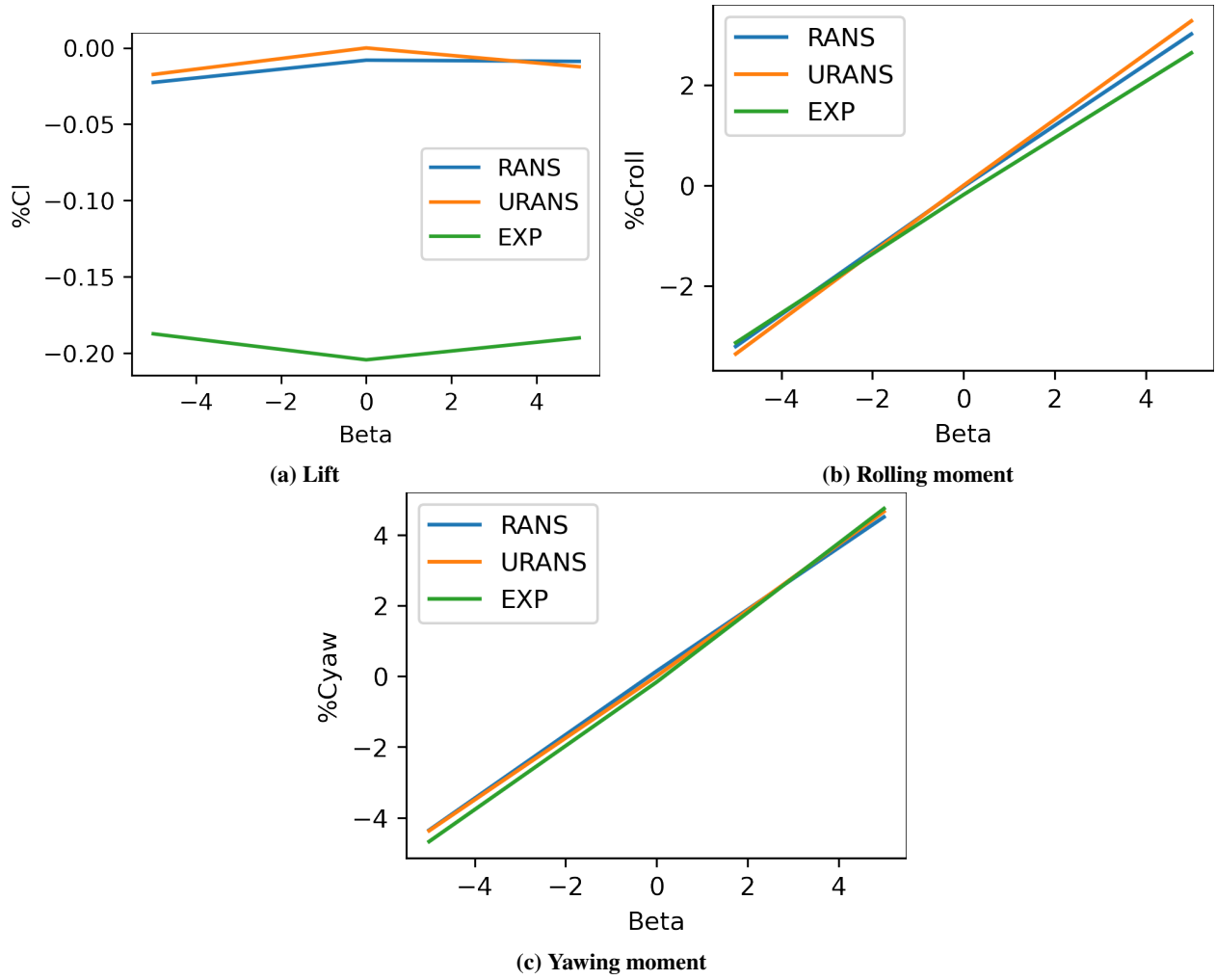


**Fig. 7** Difference in calculated force coefficients, relative to URANS results at zero side slip

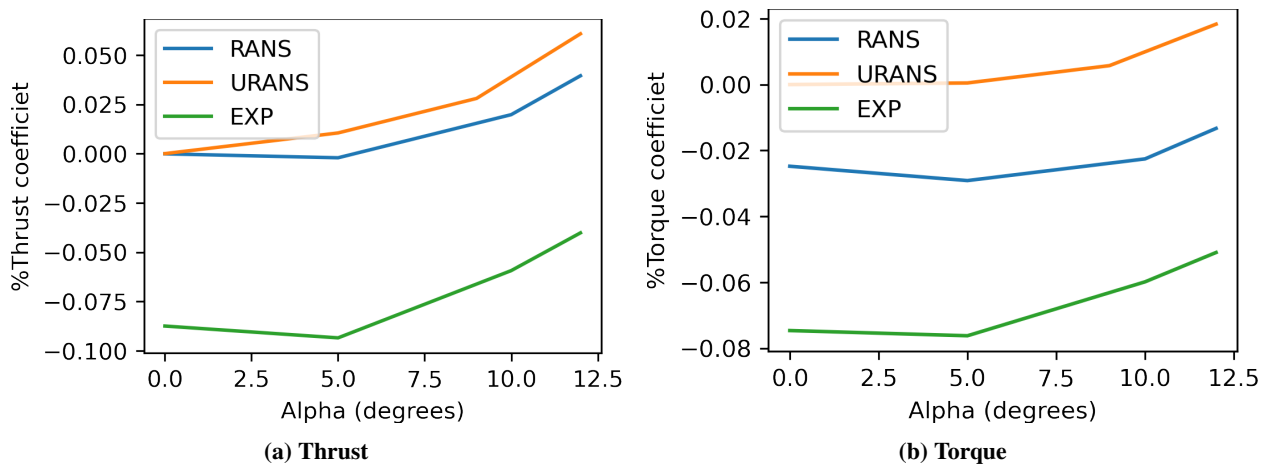


**Fig. 8** Difference in port propeller loads, relative to URANS results at zero angle of attack

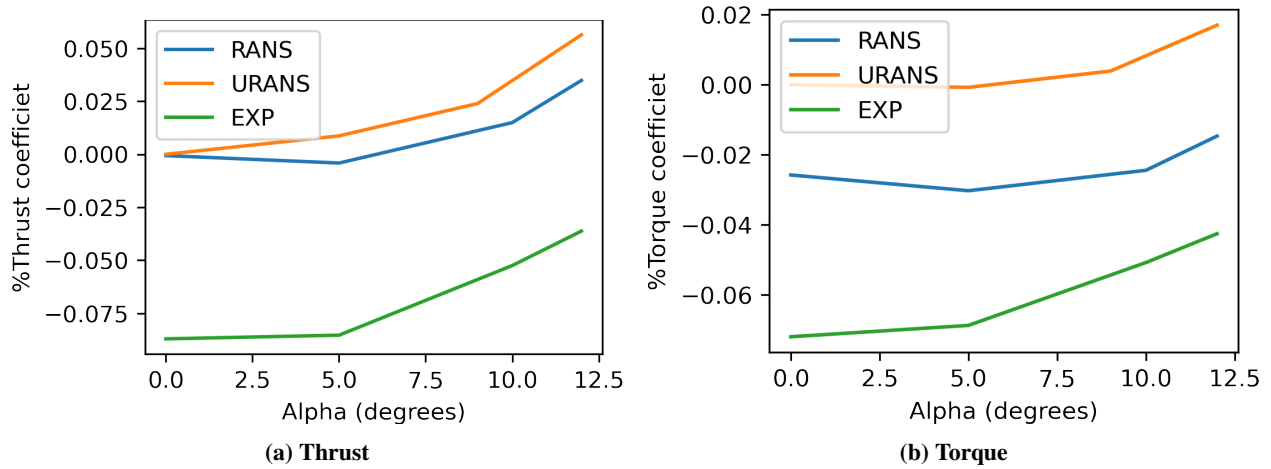


**Fig. 9** Difference in starboard propeller loads, relative to URANS results at zero angle of attack

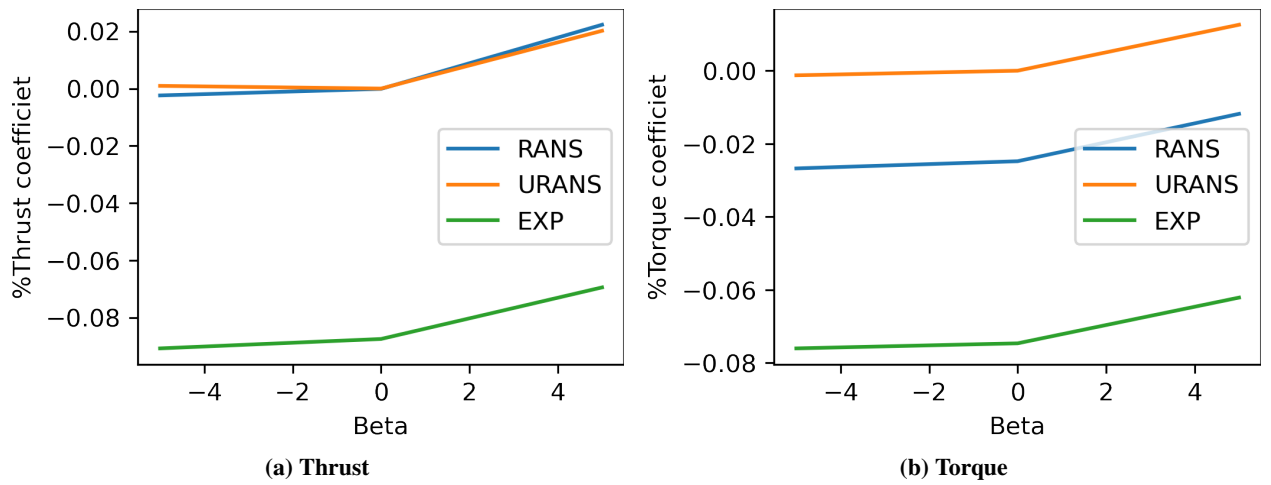


**Fig. 10** Difference in port propeller loads, relative to URANS results at zero side slip

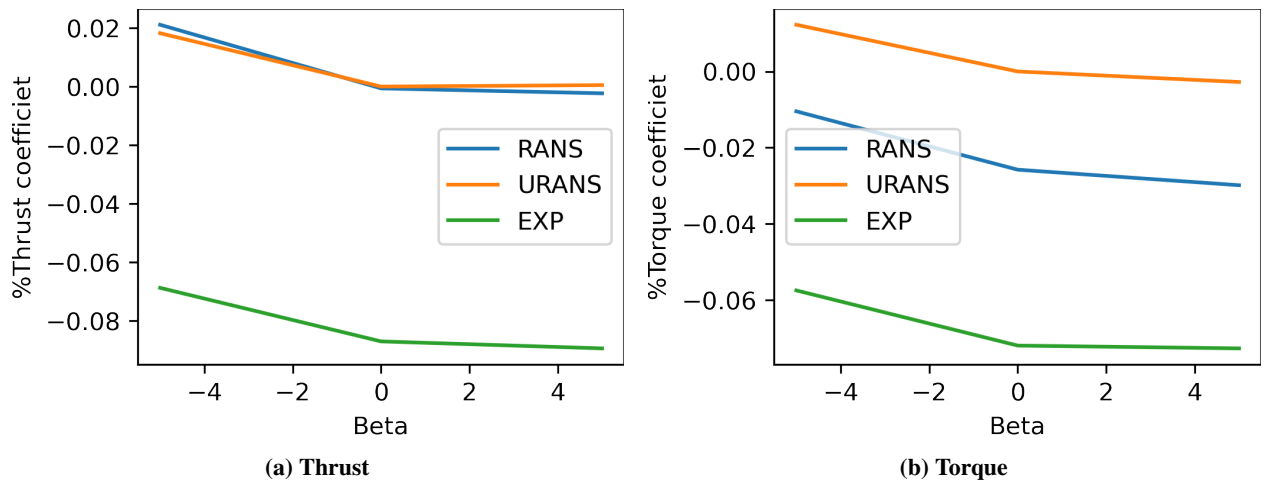


**Fig. 11** Difference in starboard propeller loads, relative to URANS results at zero side slip